

Site-selective radiation damage of collapsed carbon nanotubes

Vincent H. Crespi^{a)}

Department of Physics, 104 Davey Lab, The Pennsylvania State University, University Park, Pennsylvania 16802-6300

Nasreen G. Chopra, Marvin L. Cohen, and A. Zettl

Department of Physics, University of California at Berkeley and Materials Sciences Division, Lawrence Berkeley National Laboratory, Berkeley, California 94720

Velimir Radmilović

Department of Physical Metallurgy, University of Belgrade Karnegijeva 4, P.O. Box 494, Belgrade, 11001 Yugoslavia

(Received 2 June 1998; accepted for publication 25 August 1998)

Carbon nanotubes can flatten into collapsed tubes with bulbs along either edge. The strong anisotropy in the graphitic radiation damage threshold both explains the rapid destruction of face-on flattened nanotubes and can be exploited to selectively modify the structure of edge-on flattened nanotubes, thereby creating one-dimensional sp^2 carbon with noncontinuous transverse boundary conditions. © 1998 American Institute of Physics. [S0003-6951(98)02843-5]

A carbon nanotube¹ can collapse radially into a flattened tube with bulbs on either edge wherein the attraction between opposing sides of the inner wall outweighs the energetic cost of the increased curvature when collapsed.^{2,3} A comparison of the damage patterns in a transmission electron microscope (TEM) reveals that electron irradiation of edge-on flattened tubes can selectively remove the bulbs and yield a novel one-dimensional multilayered graphitic strip. First, we present the relevant structural features in the TEM images and image simulations of undamaged tubes before discussing experimental damage patterns and a lattice Monte Carlo model of beam damage.

The flattened nanotube of Fig. 1 turns edge-on and bends in region **A** and twists through π radians in region **B**. The lack of a central open space shows that the collapse is stabilized by interlayer attraction between opposite inner surfaces. The weaker outer contrast lines which appear as the tube tilts away from edge-on arise from tangents to a single bulb, while the more distinct inner contrast lines correspond to simultaneous tangents to both bulbs. The Moire fringes from the crossing of opposing bulbs are spaced at ~ 8 nm, consistent with the twist rate derived from the variations in apparent width (0.0018 radians per nanometer). Over the distance shown the number of high-contrast lines decreases from sixteen to eight and eight weaker outer contrast lines appear on each side of the tilting tube as the eight Moire fringes are passed. Although a rapid twist distorts the tube cross section,³ the gradual twist here should not cause significant distortion.

Image simulations used the multislice method⁴ for image simulation of small particles⁵ as implemented on the MacTempas© package.⁶ We simulated a three-walled flattened nanotube with wrapping indices (41,81), (32,97) and (43,98).⁷ Computational constraints prevent the simulation of a tube with more walls, but the essential features are visible in this tube. Continuum elasticity theory³ provided the struc-

tural details: the inner bulb is 7.8 Å in diameter; the central flat portion is 88 Å wide; the corresponding circular radius of the inner wall is 4.1 nm. We simulate a 6700-atom 2 nm long slice of tube at a range of view angles for a 400 keV JEOL 4000EX. Although only images at optimal defocus ($\sqrt{1.5C_s\lambda} = -50$ nm for $C_s = 1$ mm) are presented, results at other defocus settings aided the identification of tube features during the image analysis.

Figure 2 clearly shows the cooperative scattering from overlapping opposing bulbs and the enhancement in contrast as the tube tilts from face-on to edge-on. As in the TEM images, the innermost contrast lines are most pronounced, with weaker outer contrast lines on each side from the outer nonoverlapping bulb walls. The image at $\theta = 0.9^\circ$ shows a subtle doubling of the contrast lines as the bulbs intersperse, as seen in Fig. 1. This subtle feature is not visible in the projected potential due to averaging over a narrow band of pixels.

Previous work has shown that a circular tube is preferentially damaged on the exposed walls which have normal vectors along the beam direction.⁸ The enhanced structural anisotropy of a flattened tube yields a much more pronounced damage pattern that could be exploited to selectively modify sp^2 carbon structures on the nanoscale with a uniform irradiation. We first describe the experimental results before turning to the theoretical simulation.

When a flattened tube is edge-on to the beam, the majority of the most energetic atomic recoils occur within the graphitic plane, the direction of largest damage threshold.⁸ In fact, the image of Fig. 1 was taken after a 70-second irradiation in a flux of $2.5 \times 10^{22} \text{ m}^{-2} \text{ s}^{-1}$ 200 keV electrons; this exposure does not affect the tube-derived contrast lines compared to an earlier image (not shown). In contrast, a face-on collapsed nanotube is easily destroyed: recoils perpendicular to the sp^2 plane have the lowest damage threshold and a large fraction of the carbon atoms in a face-on tube can suffer such recoils. Figure 3 shows the rapid destruction of a flattened nanotube face-on under similar irradiation.

^{a)}Electronic mail: vhc2@psu.edu

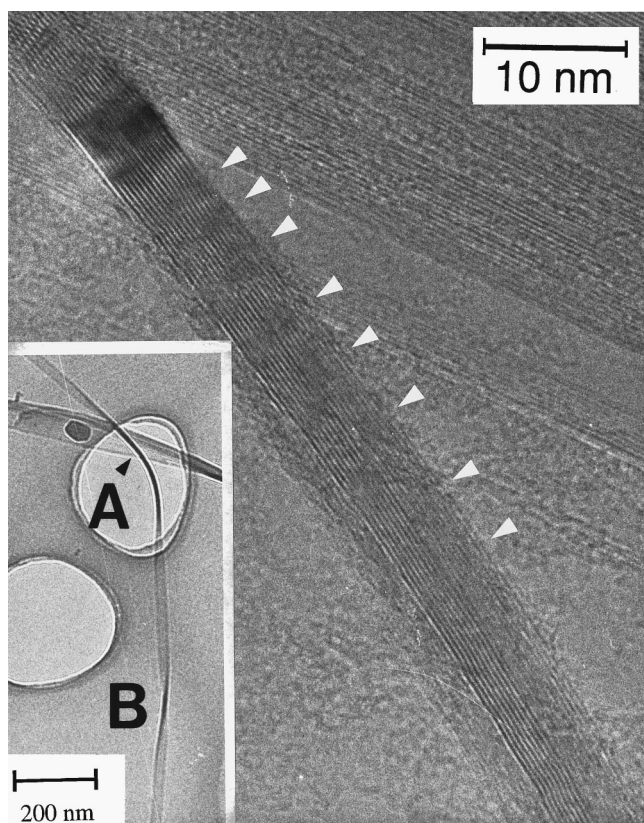


FIG. 1. This flattened nanotube turns edge-on at **A** and twists at **B**. The main figure is a high-resolution transmission electron microscopy image of region **A**. Arrows highlight lateral Moiré smudges associated with increments in the number of contrast lines. The number of contrast lines doubles in the region of highest contrast at the top of the image.

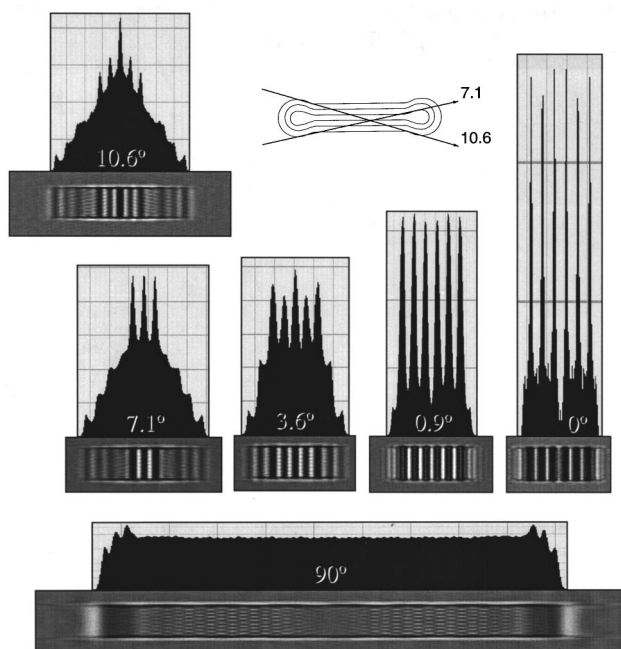


FIG. 2. Image simulations of a three-walled nanotube at different angles measured from edge-on. Upper plots show the projected potential averaged over a narrow band traversing the short dimension of the image and using the same vertical scale for each plot. Lower plots show the image simulation. Angles 7.1° and 10.6° show how cooperative scattering from the bulbs yields central lines of higher contrast. The image at 0.9° shows the subtle doubling of contrast lines just off perfect alignment. These features are seen experimentally in Fig. 1.

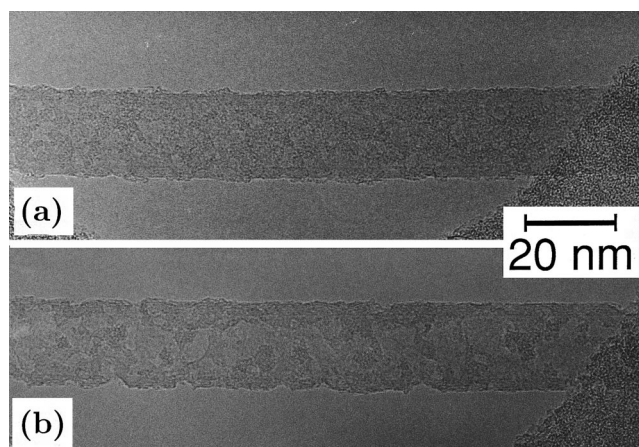


FIG. 3. Face-on flattened nanotube over the hole in the grid. Image (a) is after 30 s of exposure to a 200 keV electron beam with flux $4.6 \times 10^{22} \text{ m}^{-2} \text{ s}^{-1}$. Image (b) is after roughly 45 additional seconds of exposure. The tube is quickly destroyed.

These simple observations suggest that a uniform electron beam could perform nanoscale manipulations of anisotropic sp^2 structures. We studied such manipulations at an atomic level with a lattice Monte Carlo simulation of beam damage which places a carbon atom on each lattice site of a multiwalled flattened nanotube and computes the ejection probabilities per unit time for each atom.⁹ The ejection probability integrates the cross section for energy transfers exceeding the ejection threshold over all angles of the transferred momentum. Since the ejection threshold depends primarily on the angle between the momentum transfer and the local normal of the sp^2 sheet, we average the ejection threshold over the azimuthal angle. Previously calculated ejection thresholds for selected angles⁸ were linearly or quadratically interpolated to arbitrary angles.

In the lattice Monte Carlo simulation, ejected atoms either leave the tube or recombine immediately with the newly formed vacancy.¹⁰ A complete treatment of recombination would require long-time off-lattice dynamics and therefore lies beyond the scope of the model (for very thin structures such as flattened carbon nanotubes many of displaced atoms are ejected completely from the structure, suggesting that recombination and annealing are less important than in thicker materials such as carbon onions).¹¹ If the displaced atom encounters no obstructions in the direction of recoil, then the recombination probability is zero (an obstruction is defined as an atom within one carbon-carbon bond length of the undisturbed trajectory of the displaced atom). Under obstruction, recombination is allowed with a fixed probability from 0.1 to 0.8. This wide variation covers the uncertainties in the complex details of recombination. Fortunately, wide variations in the recombination probability do not change the essential qualitative results to be presented. Since we present only those conclusions which are unchanged under wide variation in recombination probability, we have confidence that the uncertainties in the details of recombination do not affect these conclusions.

Within the simulation, nanotubes face-on to the electron beam disintegrate quickly. An atomic ejection reduces the damage thresholds of the remaining neighbors; this positive feedback creates a mottled damage pattern. Figure 4(b)

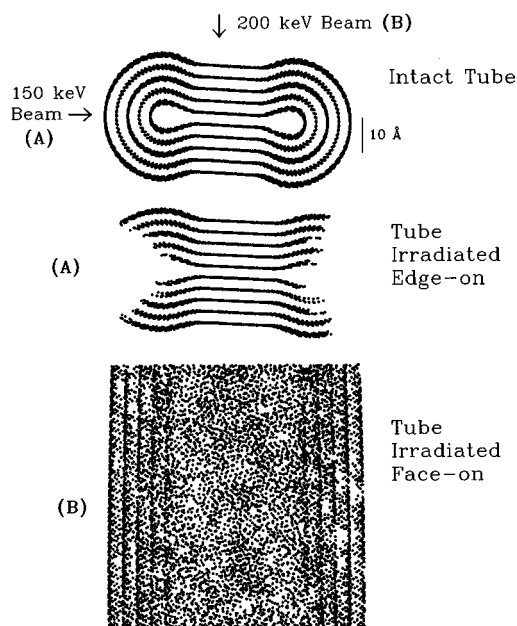


FIG. 4. Lattice Monte Carlo damage simulation of edge-on and face-on nanotubes irradiated with 150 or 200 keV electrons. The face-on tube shows a uniformly mottled damage pattern as seen in Fig. 3. The bulbs of the edge-on nanotube are completely removed, leaving a nanoscale carbon ribbon. Similar damage patterns are seen at other beam energies. The tubes have been twisted slightly for clarity.

shows the result for six-walled nanotube after irradiation face-on with 200 keV electrons at roughly 0.5 displacements per atom. The rapid, uniformly mottled damage, particularly apparent near the edges, is similar to the experimental result of Fig. 3 (but on a smaller scale in the simulation).¹²

The irradiation of edge-on tubes is more interesting and yields a controlled nanoscale structural modification of the tube. Although the bulk of the atoms in an edge-on collapsed tube are relatively resistant to ejection, the bulbs themselves disintegrate rapidly. The anisotropy in the damage pattern is maximized by tuning the beam energy so that the scattering cross section drops rapidly over the range of damage thresholds for different regions of the nanotube. Figure 4(a) shows the damage pattern for an edge-on flattened nanotube under irradiation by 150 keV electrons. This energy is above the threshold for ejection perpendicular to the sheet, but below that for near-parallel ejection. The irradiation completely destroys the bulbs, but does not affect the center. Irradiation with 200–800 keV electrons produce similar but slightly less pronounced anisotropies. Since these results depend on the qualitative distinction between parallel and perpendicular ejection, they are robust under very wide variations in the recombination efficiency for single-walled or multi-walled tubes.

Radiation damage destroys the circumferential periodicity and transforms a collapsed edge-on tube into a multilayered graphitic ribbon. Both the interlayer attraction and reconstructed interlayer covalent bonds on the edges of the ribbon (similar to those seen for open multiwalled

nanotubes¹³) will discourage disintegration by interlayer sliding. These multilayered graphitic ribbons are a larger, longer relative of directly synthesized molecular ribbons.¹⁴ Whereas regular nanotubes have periodic boundary conditions which yield semiconductors or metals depending on the wrapping indices,¹⁵ the sp^2 sheets in nanoscale ribbons contains true transverse edges. In addition to bandgaps opened from transverse quantization, certain ribbon structures exhibit novel nearly dispersionless edge states.¹⁶ Such structures could also exhibit disorder effects due to irregular edges.

In sum, the pronounced anisotropy in structural integrity under irradiation affords the ability to modify sp^2 nanostructures on the nanoscale with a uniform irradiation. In particular, tangential irradiation of edge-on flattened nanotubes can produce nanometer-wide, micron-long carbon ribbons in which the circumferential continuity has been destroyed. Although the bulbs of a flattened nanotube do not contain chemically reactive pentagons, they are still the highest curvature region of the structure; therefore these graphitic ribbons may also be producible by chemical means.

This research was supported by the National Science Foundation Grant No. DMR-9520554 and by the Office of Energy Research, Office of Basic Energy Sciences, Materials Sciences Division of the U.S. Department of Energy under Contract No. DE-AC03-76SF00098. One of the authors (A.Z.) acknowledges support from the Miller Institute for Basic Research in Science.

¹ S. Iijima, *Nature (London)* **354**, 56 (1991).

² N. G. Chopra, L. X. Benedict, V. H. Crespi, M. L. Cohen, S. G. Louie, and A. Zettl, *Nature (London)* **377**, 135 (1995).

³ L. X. Benedict, N. G. Chopra, M. L. Cohen, A. Zettl, S. G. Louie, and V. H. Crespi, *Chem. Phys. Lett.* **286**, 490 (1998).

⁴ P. Goodman and A. F. Moodie, *Acta Crystallogr., Sect. A: Cryst. Phys., Diffraction, Theor. Gen. Crystallogr.* **30**, 280 (1970).

⁵ J.-O. Malm and M. A. O'Keefe (unpublished).

⁶ Available from R. Killas, Total Resolution, Berkeley, CA.

⁷ We use the naming convention of R. Saito, M. Fujita, G. Dresselhaus, and M. S. Dresselhaus, *Appl. Phys. Lett.* **60**, 2204 (1992).

⁸ V. H. Crespi, N. G. Chopra, M. L. Cohen, and A. Zettl, *Phys. Rev. B* **54**, 5927 (1996).

⁹ In the simulation atoms are ejected individually and not, e.g., as dimers. Dimer ejection would follow similar trends with regard to anisotropy of the damage pattern.

¹⁰ Recombination with other vacancies is not allowed, but can be to a large extent subsumed within an effective recombination rate for the nacent vacancy.

¹¹ D. Ugarte, *Carbon* **33**, 989 (1995).

¹² The mottling would be enhanced if the model allowed ejection of exposed multiatom units disconnected from the rest of the structure.

¹³ J. C. Charlier, A. DeVita, X. Blase, and R. Car, *Science* **275**, 646 (1997); M. B. Nardelli, C. Brabec, A. Maiti, C. Roland, and J. Bernholc, *Phys. Rev. Lett.* **80**, 313 (1998).

¹⁴ S. Breidenbach, S. Ohren, M. Nieger, and F. Vögtle, *Chem.-Eur. J.* **2**, 832 (1996).

¹⁵ N. Hamada, S. Sawada, and A. Oshiyama, *Phys. Rev. Lett.* **68**, 1579 (1992); J. W. Mintmire, B. I. Dunlap, and C. T. White, *ibid.* **68**, 631 (1992); R. Saito, M. Fujita, G. Dresselhaus, and M. S. Dresselhaus, *Appl. Phys. Lett.* **60**, 2204 (1992).

¹⁶ K. Nakada, M. Fujita, G. Dresselhaus, and M. S. Dresselhaus, *Phys. Rev. B* **54**, 17954 (1996).